

This discussion paper is/has been under review for the journal Atmospheric Chemistry and Physics (ACP). Please refer to the corresponding final paper in ACP if available.

# Saharan dust event impacts on cloud formation and radiation over Western Europe

**M. Bangert<sup>1</sup>, A. Nenes<sup>2,3</sup>, B. Vogel<sup>1</sup>, H. Vogel<sup>1</sup>, D. Barahona<sup>4,5</sup>, V. A. Karydis<sup>2</sup>, P. Kumar<sup>3,6</sup>, C. Kottmeier<sup>1</sup>, and U. Blahak<sup>7</sup>**

<sup>1</sup>Institute for Meteorology and Climate Research, Karlsruhe Institute of Technology, Karlsruhe, Germany

<sup>2</sup>School of Earth and Atmospheric Sciences, Georgia Institute of Technology, Atlanta, GA, USA

<sup>3</sup>School of Chemical and Biomolecular Engineering, Georgia Institute of Technology, Atlanta, GA, USA

<sup>4</sup>Global Modeling and Assimilation Office, NASA GSFC, Greenbelt, MD, USA

<sup>5</sup>I.M. Systems Group, Rockville, MD, USA

<sup>6</sup>SABIC-Innovative Plastics, Selkirk, NY, USA

<sup>7</sup>Deutscher Wetterdienst, Offenbach, Germany

Received: 8 November 2011 – Accepted: 18 November – Published: 5 December 2011

Correspondence to: M. Bangert (max.bangert@kit.edu)

Published by Copernicus Publications on behalf of the European Geosciences Union.

**Saharan dust event  
impacts on cloud  
formation over  
Western Europe**

M. Bangert et al.

Title Page

Abstract

Introduction

Conclusions

References

Tables

Figures

⏪

⏩

◀

▶

Back

Close

Full Screen / Esc

Printer-friendly Version

Interactive Discussion



## Abstract

We investigated the impact of mineral dust particles on clouds, radiation and atmospheric state during a strong Saharan dust event over Europe in May 2008, applying a comprehensive online-coupled regional model framework that explicitly treats particle microphysics and chemical composition. Sophisticated parameterizations for aerosol activation and ice nucleation, together with two-moment cloud microphysics are used to calculate the interaction of the different particles with clouds depending on their physical and chemical properties.

The impact of dust on cloud droplet number concentration was found to be low, with just a slight increase in cloud droplet number concentration for both uncoated and coated dust. For temperatures lower than the level of homogeneous freezing, no significant impact of dust on the number and mass concentration of ice crystals was found, though the concentration of frozen dust particles reached up to  $100\text{ l}^{-1}$  during the ice nucleation events. Mineral dust particles were found to have the largest impact on clouds in a temperature range between freezing level and the level of homogeneous freezing, where they determined the number concentration of ice crystals due to efficient heterogeneous freezing of the dust particles and modified the glaciation of mixed phase clouds.

Our simulations show that during the dust events, ice crystals concentrations were increased twofold in this temperature range (compared to if dust interactions are neglected). This had a significant impact on the cloud optical properties which caused a reduction in the incoming short-wave radiation at the surface up to  $-75\text{ W m}^{-2}$  in areas with high dust concentrations. Including the direct interaction of dust with radiation caused an additional reduction in the incoming short-wave radiation which was found to be in the order of  $-40$  to  $-80\text{ W m}^{-2}$ . In contrast to the aerosol-cloud interaction only simulation, the incoming long-wave radiation at the surface was increased significantly in the order of  $+10\text{ W m}^{-2}$ .

## Saharan dust event impacts on cloud formation over Western Europe

M. Bangert et al.

Title Page

Abstract

Introduction

Conclusions

References

Tables

Figures



Back

Close

Full Screen / Esc

Printer-friendly Version

Interactive Discussion



The strong radiative forcings associated with dust caused a reduction in surface temperature in the order of  $-0.2$  to  $-0.5$  K for most parts of France, Germany, and Italy during the dust event. The maximum difference in surface temperature was found in the East of France, the Benelux, and Western Germany with up to  $-1$  K.

This magnitude of temperature change was sufficient to explain a systematic bias in numerical weather forecasts during the period of the dust event.

## 1 Introduction

Aerosol particles are an important part of the atmosphere. They directly modify the planetary radiation budget by scattering and absorption of long and shortwave radiation, and they affect the properties of clouds. Depending on their size and chemical composition, aerosol particles can act as cloud condensation nuclei, CCN, and ice nuclei, IN, and profoundly impacting the cloud microphysical processes and optical properties, hence the hydrological cycle and climate.

The complexity of the interactions of aerosol particles with radiation and the hydrological cycle render the most uncertain factors in climate studies and weather prediction.

One of the major contributors to the atmospheric aerosol mass is mineral dust. Even though the emission sources of mineral dust in the atmosphere are mainly desert regions, dust particles can be transported over long distances. Europe and the Mediterranean can be strongly affected by dust outbreaks originating in the Sahara Desert (Wiacek et al., 2010). Dust particles modify the atmospheric radiation balance (Cavazos et al., 2009), which can cause a cooling or heating of the surface depending on several factors like the surface albedo and the elevation of the dust layer (Stanelle et al., 2010; Cavazos et al., 2009; Yin and Chen, 2007). Including the interaction of mineral dust with radiation in model systems used for numerical weather prediction has the potential to improve the quality of the forecast, especially in regions like Europe and the Mediterranean where the dust concentrations are dominated by sporadic Saharan dust events (Perez et al., 2006; Chaboureau et al., 2011).

### Saharan dust event impacts on cloud formation over Western Europe

M. Bangert et al.

Title Page

Abstract

Introduction

Conclusions

References

Tables

Figures

⏪

⏩

◀

▶

Back

Close

Full Screen / Esc

Printer-friendly Version

Interactive Discussion





**Saharan dust event  
impacts on cloud  
formation over  
Western Europe**

M. Bangert et al.

Title Page

Abstract

Introduction

Conclusions

References

Tables

Figures

⏪

⏩

◀

▶

Back

Close

Full Screen / Esc

Printer-friendly Version

Interactive Discussion



The impact of dust on the cloud droplet concentration in most studies was hypothesized to be caused by hygroscopic coatings, which make them important CCN due to their large size. With the exception of dust from dry lake beds, freshly emitted dust contains little soluble material (Kumar et al., 2011). Processing of dust particles in clouds (Levin et al., 1996) and the condensation of acids on the particles (Sullivan et al., 2007) are prime mechanisms thought of creating hygroscopic coatings on dust. Kumar et al. (2011) however pointed out that dust particles do not require deliquescent material to act as CCN in the atmosphere, as the adsorption of water on the particle can induce hygroscopicity equivalent to having a considerable soluble fraction. In a global study, Karydis et al. (2011) pointed out that even uncoated mineral dust can contribute significantly to cloud droplet number close to the source regions and that hygroscopic coating of dust particles can decrease the cloud droplet number in regions which are affected by anthropogenic emissions due to a decrease in water supersaturation.

This study focuses on a major dust event that occurred in May 2008. Its origin was in the Sahara and from there mineral dust particles were transported over the Western Mediterranean, covering large areas of Western Europe. During the episode, high aerosol concentrations were observed throughout Europe; ice nuclei concentrations significantly increased (compared to pre-event levels) at Kleiner Feldberg, Germany (Klein et al., 2010). During this time, traditional weather forecast models exhibited poor prediction skill. The German national meteorological service (Deutscher Wetterdienst, DWD) detected a significant bias in their numerical weather forecast of the 2-m temperatures of +1.5K when the dust outbreaks reached SW-Germany (Darrath, 2010, DWD, personal communication). The operational weather forecast at DWD is performed with the model system COSMO (Consortium for Small-scale Modeling) (Baldauf et al., 2011). Since the impact of aerosol particles on atmospheric state is accounted for in COSMO by using prescribed profiles for aerosol optical properties and prescribed cloud droplet and ice crystal numbers, extraordinary aerosol conditions like the dust event in May 2008 are not represented in the simulations. This can potentially cause biases in the weather forecast.

---

## Saharan dust event impacts on cloud formation over Western Europe

M. Bangert et al.

---

[Title Page](#)[Abstract](#)[Introduction](#)[Conclusions](#)[References](#)[Tables](#)[Figures](#)[⏪](#)[⏩](#)[◀](#)[▶](#)[Back](#)[Close](#)[Full Screen / Esc](#)[Printer-friendly Version](#)[Interactive Discussion](#)

The impacts of dust on atmospheric state are studied with the regional scale online-coupled model system COSMO-ART (Vogel et al., 2009) that accounts for feedbacks between chemistry, aerosols, radiation, and clouds. A two-moment cloud microphysics scheme (Seifert and Beheng, 2006) is coupled together with comprehensive parameterizations for aerosol activation (Kumar et al., 2009; Barahona et al., 2010a) and ice nucleation (Barahona and Nenes, 2009b) to simulate the impact of the various aerosol particles on the cloud microphysics and therefore on cloud properties and precipitation. This framework can quantify the impact of dust on atmospheric state, as it considers the competition of dust with other aerosol particles during cloud formation and the feedback processes related to cloud microphysics, radiation, and precipitation. The framework is also used to thoroughly study the sensitivity of predicted atmospheric state to the dust amount, properties (hygroscopicity), and parameterization.

## 2 The model framework

The online-coupled regional model system COSMO-ART was extended with two-moment cloud microphysics and comprehensive parameterizations for aerosol activation and ice crystal nucleation. COSMO-ART is based on the operational weather forecast model COSMO (Baldauf et al., 2011) of the Deutscher Wetterdienst (DWD) which was online coupled with comprehensive modules for gas phase chemistry and aerosol dynamics. An extended version of MADEsoot (Riemer et al., 2003) is used to represent the aerosol population with seven overlapping lognormal modes. Five modes represent sub-micron particles consisting of sulphate, ammonium, nitrate, organic compounds, water, and soot in a range of mixing states, and are allowed to interact with anthropogenic emissions of particles and gases. Sea salt and mineral dust particles are represented by three modes (Table 2). The model includes a comprehensive photochemical module to capture the temporal and spatial distributions of inorganic and semi-volatile organic compounds. The emissions of sea salt and mineral dust particles are calculated online in the model as a function of atmospheric state,

10 m-windspeed, and friction velocity, and surface properties, such as sea surface temperature, soil type, and soil moisture (Lundgren, 2010; Stanelle et al., 2010). A detailed description of the treatment of gases, aerosols, and their emissions is given by Vogel et al. (2009).

## 5 2.1 Cloud microphysics

COSMO includes an efficient bulk cloud microphysics scheme, designed for operational weather forecast (Doms et al., 2005). This scheme cannot treat aerosol-cloud interactions, because only one moment of the size distribution is calculated. Bangert et al. (2011) extended the cloud scheme to a two-moment representation of the cloud droplet size distribution to consider the impact of aerosol particles on warm cloud microphysics. To further improve the clouds microphysics and to enable the simulation of aerosol impacts on ice clouds a comprehensive two-moment bulk microphysical scheme (Seifert and Beheng, 2006; Seifert et al., 2006; Noppel et al., 2006; Blahak, 2008) was introduced, which replaces the old schemes. This scheme distinguishes six hydrometeor categories (cloud drops, cloud ice, rain, snow, graupel, and hail) and represents each particle type by its respective number and mass concentration. A (generalized) gamma size distribution is used for each hydrometeor class, where the so-called shape parameters are held constant during the simulation. For the warm clouds, the scheme considers autoconversion of cloud droplets to rain, accretion of cloud droplets by rain drops, self-collection of cloud and rain droplets, break-up of rain drops, and evaporation of rain drops. Condensational growth of cloud droplets is calculated with a saturation adjustment technique. For the cold clouds, homogeneous and heterogeneous ice nucleation, diffusional growth of ice crystals, freezing of cloud and rain droplets, aggregation, self-collection, riming, conversion to graupel, melting, sublimation, shedding, and Hallett-Mossop ice multiplication are considered. The freezing of cloud and rain drops is calculated with a classical statistical approach based on an empirical relation for the freezing probability as a function of temperature (Seifert and Beheng, 2006). Note that the freezing of cloud and rain droplets is independent of

## Saharan dust event impacts on cloud formation over Western Europe

M. Bangert et al.

Title Page

Abstract

Introduction

Conclusions

References

Tables

Figures

⏪

⏩

◀

▶

Back

Close

Full Screen / Esc

Printer-friendly Version

Interactive Discussion



the simulated IN concentrations. This may introduce an underestimation of the glaciation of mixed phase clouds for high IN concentrations, but can be justified by a small fraction of cloud droplets originating from activated dust particles in our simulations. A detailed description of the cloud microphysical processes is given in Seifert and Beheng (2006), and a statistical analysis of the aerosol-cloud interaction for three summer seasons using the microphysics scheme is presented in Seifert et al. (2011).

Although COSMO is a non-hydrostatic model and therefore permits the simulation of convection, a parameterization of subgrid-scale deep convection has to be used for coarse model resolutions. We use a modified Tiedtke scheme (Tiedtke, 1989) for horizontal resolutions coarser than 7 km, which considers the convective transport of gases and aerosol particles.

## 2.2 Aerosol activation

The activation of an aerosol particle to a clouds droplet depends on its ability to remain in a stable equilibrium with the ambient water vapor. The water vapor saturation ratio,  $S_{\text{eq}}$ , of an aerosol particle in equilibrium with surrounding water vapor can be expressed as

$$S_{\text{eq}} = \alpha_w e^{\frac{4\sigma M_w}{RT\rho_w D}}, \quad (1)$$

where  $\sigma$  is the surface tension at the particle-gas interface,  $M_w$  is the molar mass of water,  $R$  is the universal gas constant,  $T$  is the temperature,  $\rho_w$  is the density of water, and  $D$  is the equivalent particle diameter. The exponential in Eq. (1) is commonly referred to as the curvature or Kelvin effect.  $\alpha_w$  is the activity of the water and depends on the physiochemical properties of the particle. In case of a soluble aerosol particle  $\alpha_w$  can be expressed by the effective mole fraction of water in the solution droplet, which results in the well known Köhler equations. For insoluble particles, e.g. dust, this classical theory cannot be applied, because  $S_{\text{eq}}$  is now affected by another physical process namely the process of physisorption of water vapor on the particle surface. In

### Saharan dust event impacts on cloud formation over Western Europe

M. Bangert et al.

Title Page

Abstract

Introduction

Conclusions

References

Tables

Figures

⏪

⏩

◀

▶

Back

Close

Full Screen / Esc

Printer-friendly Version

Interactive Discussion



this case  $\alpha_w$  can be determined by FHH (Frenkel, Halsey, and Hill) adsorption theory (e.g. Lowell et al., 2004)

$$\alpha_w = e^{-A_{FHH}\Theta^{-B_{FHH}}}, \quad (2)$$

where  $A_{FHH}$ ,  $B_{FHH}$  are empirical constants, and  $\Theta$  is the surface coverage (defined as the number of adsorbed layers of water).  $A_{FHH}$  characterizes interactions of adsorbed molecules with the aerosol surface and adjacent adsorbate molecules (i.e., those in the first monolayer).  $B_{FHH}$  characterizes the attraction between the aerosol surface and the adsorbate in subsequent layers; the smaller the value of  $B_{FHH}$ , the greater the distance at which the attractive forces act (Sorjamaa and Laaksonen, 2007).  $A_{FHH}$  and  $B_{FHH}$  are compound-specific and determined experimentally. Both theories (Köhler and FHH) show a similar behavior for  $S_{eq}$ , with a characteristic maximum (the critical supersaturation  $s_c$ ). For ambient supersaturations greater than  $s_c$  the particle can get activated and grow to the size of a cloud droplet.

In this study we use a comprehensive activation parameterization (Kumar et al., 2009; Barahona et al., 2010a) based on a cloud parcel framework, in which a parcel of air containing an external mixture of Köhler and FHH particles is lifted. At first the  $s_c$  distribution is calculated for each aerosol. Then the supersaturation equation of the parcel is solved using the bisection method to determine the maximum supersaturation,  $s_{max}$ , and the number of activated particles,  $N_a^*$ . As input data the simulated cloud-scale dynamics (updraft, temperature, pressure) and aerosol properties (size distributions and chemical compositions of all aerosol modes) are used.

To account for hygroscopic coating of e.g. dust particles, Kumar et al. (2011) developed a unified activation theory by merging Köhler and FHH theory in their parameterization. For coated dust particles  $\alpha_w$  is represented by

$$\alpha_w = x_w e^{-A_{FHH}\Theta^{-B_{FHH}}}, \quad (3)$$

where  $x_w$  is the mole fraction of water in the droplet and represents the solute effects on water activity.

## Saharan dust event impacts on cloud formation over Western Europe

M. Bangert et al.

Title Page

Abstract

Introduction

Conclusions

References

Tables

Figures

⏪

⏩

◀

▶

Back

Close

Full Screen / Esc

Printer-friendly Version

Interactive Discussion



Based on the procedure of Bangert et al. (2011) the activation rate, ACT, of aerosol particles in the model is calculated in different ways, replacing the activation rate in Eq. (17) of Seifert and Beheng (2006). For a newly formed cloud the parameterization is directly applied and  $N_a^*/\Delta t$  equals the activation rate, where  $\Delta t$  is the time step used.

In case of an already existing cloud the activation rate at the cloud base is calculated on the basis of advection and turbulent diffusion of particles into the cloud base

$$\text{ACT} = -\frac{\partial}{\partial z} N_a^*(s_{\max}) w + \frac{\partial}{\partial z} K \frac{\partial}{\partial z} N_a^*(s_{\max}), \quad (4)$$

where  $w$  is the grid-scale updraft,  $z$  is the height above sea level, and  $K$  is the turbulent diffusion coefficient.

In-cloud activation is calculated, if the simulated grid-scale supersaturation increases again above the cloud base, e.g. from strong updrafts. In this case the growth of the existing cloud droplets is considered by assuming they act as giant CCN that deplete supersaturation by the approach of Barahona et al. (2010a). The corresponding activation rate is calculated as  $N_a^*/\Delta t$ .

### 2.3 Ice nucleation

The nucleated number concentration of ice crystals,  $N_i^*$ , is calculated using the parameterization of Barahona and Nenes (2008, 2009a,b), which is based on the framework of an ascending Lagrangian air parcel. Competition between homogeneous and heterogeneous freezing is explicitly considered in the calculation of the ice supersaturation,  $s_i$ . In doing so the dependency of  $N_i^*$  on the conditions of cloud formation (i.e.,  $T$ ,  $p$ ), updraft velocity, deposition coefficient, and soluble and insoluble aerosol concentrations is explicitly resolved.  $N_i^*$  is given by

$$N_i^* = \begin{cases} N_{\text{hom}} + N_{\text{het}}(s_{\text{hom}}); & N_{\text{het}}(s_{\text{hom}}) < N_{\text{lim}} \\ N_{\text{het}}(s_{i,\max}); & N_{\text{het}}(s_{\text{hom}}) \geq N_{\text{lim}} \end{cases}, \quad (5)$$

where  $s_{i,\max}$  is the maximum supersaturation that develops in the cirrus,  $s_{\text{hom}}$  is the homogeneous freezing threshold (Koop et al., 2000), and  $N_{\text{hom}}$  and  $N_{\text{het}}$  are the number

**Saharan dust event impacts on cloud formation over Western Europe**

M. Bangert et al.

Title Page

Abstract

Introduction

Conclusions

References

Tables

Figures

⏪

⏩

◀

▶

Back

Close

Full Screen / Esc

Printer-friendly Version

Interactive Discussion



## Saharan dust event impacts on cloud formation over Western Europe

M. Bangert et al.

Title Page

Abstract

Introduction

Conclusions

References

Tables

Figures

◀

▶

◀

▶

Back

Close

Full Screen / Esc

Printer-friendly Version

Interactive Discussion



of ice crystals forming from homogeneous and heterogeneous freezing, respectively.  $N_{\text{lim}}$  is the IN concentration that completely inhibits homogeneous nucleation and sets the limit between combined heterogeneous-homogeneous freezing and pure heterogeneous freezing only.  $N_{\text{lim}}$  is explicitly calculated as a function of cloud formation conditions and is related to the slope of the IN spectrum,  $N_{\text{het}}(s_i)$  (Barahona and Nenes, 2009a).

The heterogeneous freezing spectrum of Phillips et al. (2008) is used for  $N_{\text{het}}(s_i)$ , which is derived from several field campaign data sets. It provides the contribution of individual aerosol species (dust, black carbon, and organics) and freezing mechanisms (e.g. immersion and deposition) to  $N_{\text{het}}(s_i)$ . The contribution of the individual dust modes to  $N_{\text{het}}(s_i)$  is scaled to their surface area distribution (Barahona and Nenes, 2009a). Niemand et al. (2011) compared different parameterizations of immersion freezing of dust. They showed that applying the heterogeneous freezing spectrum of Phillips et al. (2008) on dust concentrations simulated with COSMO-ART the measured IN concentrations at Kleiner Feldberg during the dust event were reproduced.

The homogeneous contribution to  $N_i^*$  is given by

$$N_{\text{hom}} = \begin{cases} N_0 e^{-f_c} (1 - e^{-f_c}) & f_c < 0.6 \\ N_0 \left[ 1 + e^{\left(\frac{9-2f_c}{7}\right)} \right]^{-1} & f_c \geq 0.6 \end{cases}, \quad (6)$$

where  $N_0$  is the number concentration of the supercooled liquid droplet population and  $f_c$  is the droplet freezing fraction for cirrus clouds formed in situ (Barahona and Nenes, 2008).  $N_0$  equals the sum of the number concentration of the soluble aerosol modes (Table 2) which are assumed to deliquesce during ice cloud formation.

The nucleation rate of ice crystals, NUC, is calculated following Seifert and Beheng (2006) Eq. (34) by

$$\text{NUC} = \max\left(\frac{N_i^* - N_i}{\Delta t}, 0\right), \quad (7)$$

where  $N_i$  is the number concentration of ice crystals before the nucleation pulse.

## 2.4 Subgrid-scale updrafts

Though regional models are able to resolve individual cloud systems, they cannot explicitly capture the updraft velocities which control nucleation of ice and droplets. Therefore parameterizations of the subgrid-scale vertical velocity must be applied to address this issue.

Sub-grid scale vertical velocities,  $w'$ , are described with a Gaussian probability distribution function,  $P_w(w')$ . The mean of  $P_w(w')$  is set equal to the grid scale updraft,  $w$ , and the standard deviation,  $\sigma_w$ , is calculated as the square root of the turbulent kinetic energy (Morales and Nenes, 2010). A weighted mean of the activated particles/nucleated ice crystals,  $N_x^*$ , is calculated by numerically calculating the integral

$$N_x^* = \frac{\int_0^\infty N_x^*[s_{\max}(w')]P_w(w')dw'}{\int_0^\infty P_w(w')dw'}. \quad (8)$$

## 2.5 Radiation

The radiative fluxes are calculated with the GRAALS (Ritter and Geleyn, 1992) radiation scheme of COSMO for eight spectral bands. To consider the impact of varying aerosol and clouds the necessary optical properties, as they are the extinction coefficient, single scattering albedo, and asymmetry factor, have to be calculated.

The optical properties of the aerosol particles are calculated as a function of the size distributions, the chemical composition, as well as the soot and water content with the parameterizations of Vogel et al. (2009), Lundgren (2010), and Stanelle et al. (2010).

To consider the varying droplet and ice crystal size in the radiation scheme the parameterizations of Hu and Stamnes (1993) and Edwards et al. (2007) are applied to calculate the optical properties of the cloud droplets and ice crystals. Here the effective radii of clouds droplets,  $r_c$ , and ice crystals,  $r_i$ , are calculated as the ratio of the third

### Saharan dust event impacts on cloud formation over Western Europe

M. Bangert et al.

Title Page

Abstract

Introduction

Conclusions

References

Tables

Figures

⏪

⏩

◀

▶

Back

Close

Full Screen / Esc

Printer-friendly Version

Interactive Discussion



to second moment of the respective size distribution. The adaption of the parameterizations for the eight spectral bands of GRAALS is carried out following Zubler et al. (2011). Precipitating hydrometeors of snow, graupel, and rain, are not considered in the radiation calculations, which may introduce a bias in the calculated radiation fields (Waliser et al., 2011).

### 3 Simulation setup

A nesting approach is used for the simulations. At first a simulation for a domain D0 covering Northwest Africa and Western Europe was performed. This domain enables the explicit simulation of the dust emissions over Africa and the long-range transport of the dust particles to Europe (Fig. 1). All gases and aerosol particles are simulated (see Sect. 2), but are not allowed to interact with clouds and radiation. Calculations of the cloud microphysical processes are carried out with the one-moment cloud scheme, which includes cloud water, rain, cloud ice, snow, and graupel. The grid size is  $0.25^\circ$  ( $\approx 28$  km) in both horizontal directions with 40 non-equidistant levels in the vertical up to an height of 20 km. Initial and boundary conditions for meteorological variables are obtained from the IFS ECMWF analysis; for gas-phase compounds, MOZART-4 results (Emmons et al., 2010) are used. Clear air conditions are assumed for the initial aerosol and for aerosol outside of the domain. The simulation starts at 22 May 2008, 00:00 UTC and ends 30 May 2008, 00:00 UTC.

For the analysis of the aerosol-cloud interaction three simulations were carried out on the nested grid for domain D1 (Fig. 1) covering regions affected by the dust event (France, Germany, and the Mediterranean). Cloud microphysical processes were simulated with the two-moment scheme (Sect. 2.1) and full interaction with the aerosol particles were allowed. The horizontal grid size is  $0.0625^\circ$  ( $\approx 7$  km) in both directions with 40 non-equidistant levels in the vertical up to an height of 20 km and the simulated period is 22 May, 00:00 UTC till 30 May, 00:00 UTC. The boundary and initial conditions for all prognostic variables are taken from the simulation of the coarse grid for domain

## Saharan dust event impacts on cloud formation over Western Europe

M. Bangert et al.

Title Page

Abstract

Introduction

Conclusions

References

Tables

Figures



Back

Close

Full Screen / Esc

Printer-friendly Version

Interactive Discussion



## Saharan dust event impacts on cloud formation over Western Europe

M. Bangert et al.

Title Page

Abstract

Introduction

Conclusions

References

Tables

Figures

⏪

⏩

◀

▶

Back

Close

Full Screen / Esc

Printer-friendly Version

Interactive Discussion



D0, which includes the concentration of dust transported from North Africa. The first four days (22 May till 25 May 2008) of the simulation are used to build up the aerosol concentration based on direct emissions and secondary formation. The analysis of the results focuses on the dust event (26 May till 29 May 2008). The individual nested simulations differ in the setup used for the dust-atmosphere interaction. In simulation REF the interaction of dust particles with clouds and radiation was not allowed. To investigate the impact of the dust particles due to their interaction with clouds we carried out simulation *C* which includes the impact of the dust particles on cloud formation via activation of dust particles and heterogeneous nucleation of cloud ice on the dust particles. In simulation *C* dust particles are assumed to not have a hygroscopic coating. Therefore the FHH adsorption theory is used for the activation of the dust particles using  $A_{\text{FHH}} = 2.5$ , and  $B_{\text{FHH}} = 1.2$  (Kumar et al., 2011). Aged dust particles can potentially have hygroscopic coatings which decreases the supersaturation needed for their activation. For this simulation *C\** is carried out, assuming that the dust particles are coated by 10% ammonium sulfate (in volume). In this case the activation of the dust particles is calculated with the unified approach of Kumar et al. (2011). In simulation CR, the direct interaction of the dust particles with long and shortwave radiation is considered additionally to their impact on cloud formation (with the conditions of simulation *C*). Table 1 gives an overview of the individual simulations and their abbreviations.

In all simulations a detailed data set for anthropogenic emissions, which includes traffic emissions, emissions by large point sources, and area sources such as households and industrial areas, is used. The emission data has an hourly resolution and includes the emission of  $\text{SO}_2$ , CO,  $\text{NO}_x$ ,  $\text{NH}_3$ , 32 individual classes of VOC, and the direct emission of elemental carbon particles (Pregger et al., 2007).

## 4 Results

During the 26 to 30 May 2008 Europe was affected by a strong Saharan dust event. A persistent trough reaching from Iceland to Morocco dominated the synoptic situation

during these days. Due to steady southerly winds over the Mediterranean dust particles were transported efficiently from the emission sources in the Sahara to Central Europe. Figure 2 shows the measured and simulated aerosol mass concentration of particles with a diameter below  $10\ \mu\text{m}$  ( $\text{PM}_{10}$ ) at Hohenpeissenberg, Germany (H. Flentje 2010, DWD, personal communication). The measurements show a strong increase of the aerosol mass starting at 26 May and lasting till 30 May. The simulation attribute this to the arrival of mineral dust transported from the Sahara. The model reproduces the measured  $\text{PM}_{10}$  concentrations reasonably well during the dust event and captures the existing aerosol background before the arrival of the dust which is dominated by particles from anthropogenic sources. Upon the arrival of the dust, the simulated  $\text{PM}_{10}$  concentration of anthropogenic and biogenic particles decrease from  $6\ \mu\text{g m}^{-3}$  to  $1\ \mu\text{g m}^{-3}$  and increase again after the dust event. This indicates that the aerosol population during a Saharan dust event over Europe differs strongly from the simple assumption of adding additional dust particles to a typical (continental) aerosol population. Therefore aerosol particles have to be simulated explicitly on the basis of anthropogenic and natural emissions in studies, which address the interaction of dust events with the atmosphere.

At the Atlas mountains the transported dust particles were lifted to the upper troposphere. This ascending air flow on the one hand enabled the long range transport of the dust particles to Central Europe and on the other hand caused conditions favorable of heterogeneous and homogeneous ice cloud formation. Additionally, warm and mixed phase clouds were formed over the whole domain.

Figure 3 presents satellite retrievals of MODIS (Menzel et al., 2008) and calculated cloud top temperatures on basis of simulation *C* during the morning hours. The cloud top temperature at the individual grid points are calculated as the temperature of the highest model layer in which the grid scale cloud optical thickness exceeds 0.05. Even though both cloud top temperatures are derived in very different ways, we make a coarse comparison if the main features of the cloud distribution are represented in the simulation. On the morning of the 26 May 2008 the high clouds in the eastern

## Saharan dust event impacts on cloud formation over Western Europe

M. Bangert et al.

[Title Page](#)[Abstract](#)[Introduction](#)[Conclusions](#)[References](#)[Tables](#)[Figures](#)[⏪](#)[⏩](#)[◀](#)[▶](#)[Back](#)[Close](#)[Full Screen / Esc](#)[Printer-friendly Version](#)[Interactive Discussion](#)



The upper layer, which reaches from the level of homogeneous freezing up to 15 km height and hence is favorable of combined homogeneous and heterogeneous freezing, has mean dust concentrations in the order of  $1 \text{ cm}^{-3}$  over Europe.

## 4.2 Dust impact on cloud droplet and ice crystal number concentration

Owing to their size and surface properties dust particles can act as CCN. High dust concentrations can therefore modify the cloud droplet size distribution and consequently the microphysical processes in the warm cloud phase. Dust particles are found to be very efficient ice crystal nuclei in several lab and field studies (Field et al., 2006; Möhler et al., 2006). Ice nucleation due to immersion freezing of dust particles starts at temperature around 263 K with a freezing fraction on the order of 0.1 %. At temperature around 253 K, the freezing fraction of dust particles was found to be in the order of 1 % (Phillips et al., 2008). At temperatures below 235 K ice crystal nucleation due to homogeneous freezing of aerosol droplets sets in. At this temperature range heterogeneous freezing of the dust particles has to compete with homogeneous freezing for water vapor.

In Fig. 5 joint histograms of cloud droplet and ice crystal number,  $N_c$  and  $N_i$ , and mass concentrations,  $m_c$  and  $m_i$ , are shown for different temperature ranges for simulation REF and C. The histograms are calculated for all grid points and the whole period of the dust event (26–29 May 2008). With the help of the joint histograms, systematic differences in the distribution of  $N_c$ ,  $N_i$ ,  $m_c$ , and  $m_i$  between the simulations can be identified together with difference in the overall number of grid points containing cloud water and ice crystals in the individual simulations.

For temperatures above freezing level, the domain-wide joint histograms of cloud droplets in simulation REF and C show small differences. This is because the overall number concentration of available CCN is dominated by sea salt and secondary aerosol particles. The number concentrations of activated dust particles,  $N_d^*$ , is mostly below  $3 \text{ cm}^{-3}$  and higher number concentrations up to  $20 \text{ cm}^{-3}$  occurred only for total

### Saharan dust event impacts on cloud formation over Western Europe

M. Bangert et al.

Title Page

Abstract

Introduction

Conclusions

References

Tables

Figures

⏪

⏩

◀

▶

Back

Close

Full Screen / Esc

Printer-friendly Version

Interactive Discussion



activated number concentrations,  $N_a^*$ , below  $200\text{ cm}^{-3}$ . The fraction of  $N_d^*$  to  $N_a^*$  is mostly below 10 %.

Despite the fact that the coated dust particles can be activated at lower supersaturations than the uncoated particles, the domain wide joint histogram of cloud droplets in simulation  $C^*$  shows only slightly higher  $N_c$  in comparison with simulation  $C$  (Fig. 5). One reason is that even though much more dust particles get activated in simulation  $C^*$  in comparison to simulation  $C$  the number is still low in comparison to the total number of activated particles for most of the grid points (Fig. 6). But we also want to point out here, that there are more cloudy grid points in simulation  $C^*$  where  $N_d^*$  contributes to 10 % or more of  $N_a^*$  at values of  $N_a^*$  below  $200\text{ cm}^{-3}$ . Hence the dust particles can have a significant impact on individual clouds for conditions with low number concentrations of other aerosol particles. Another reason for the low impact of coated dust particles on  $N_c$  is that the increased number of activated dust particles causes lower maximum supersaturations,  $s_{\max}$ , due to the growth of the dust particles. This lower supersaturation can result in a decrease of the activated droplets from aerosols other than dust. This can buffer the impact of the increased number of activated dust particles on  $N_c$  (Kumar et al., 2009) and can be another reason of why total droplet number does not increase significantly in simulation  $C^*$ . In Fig. 7 the joint histogram of the maximum supersaturation and the updraft during the activation process are shown for the cases REF,  $C$ , and  $C^*$ . The impact on  $s_{\max}$  is strongest in case  $C^*$ , with significantly lower  $s_{\max}$  in comparison to case REF. For uncoated dust particles (case  $C$ ) the impact on  $s_{\max}$  is lower, because of the small amounts of water required for FHH activation (Kumar et al., 2009), in comparison to the Köhler activation of hygroscopic particles.

The impact of the dust particles on number and mass concentration of cloud droplets and ice crystals for atmospheric layers with temperatures in the range of 273 to 235 K is dominated by the heterogeneous nucleation of ice crystals from dust particles. The joint histogram of number concentrations of ice crystals,  $N_i$ , and mass concentrations of ice crystals,  $m_i$ , show a systematic increase in  $N_i$  of  $30\text{ l}^{-1}$  which corresponds to an increase of  $N_i$  in the order of 100 % (Fig. 5). A  $N_i$  increase of the order  $30\text{ l}^{-1}$  corresponds

## Saharan dust event impacts on cloud formation over Western Europe

M. Bangert et al.

Title Page

Abstract

Introduction

Conclusions

References

Tables

Figures



Back

Close

Full Screen / Esc

Printer-friendly Version

Interactive Discussion





grid points where  $N_{\text{het}}$  exceeds  $N_{\text{lim}}$  for conditions with  $N_{\text{lim}}$  lower than  $60\text{ l}^{-1}$ . In the latter simulation,  $N_{\text{het}}$  is generally much higher due to the heterogeneous freezing of the dust particles, but rarely exceeds  $100\text{ l}^{-1}$ . Therefore  $N_{\text{het}}$  is mostly below  $N_{\text{lim}}$  and is not able to significantly impact  $N_i$ . For relatively few conditions (with  $N_{\text{lim}}$  lower than  $100\text{ l}^{-1}$ )  $N_{\text{het}}$  is able to exceed  $N_{\text{lim}}$ .

### 4.3 Dust impact on cloud properties and radiation

In the previous section we focused on the net impact of the dust particles on cloud droplet and ice crystal number concentration for the whole model domain during the simulation period and found systematically higher values in ice crystal number concentration for atmospheric layers between freezing level and the level of homogeneous freezing in case *C* in comparison to case REF. This has numerous consequences on cloud properties. We already discussed the more effective glaciation of mixed phase clouds in simulation *C*, which has potential consequences on the vertical distribution of the latent heat release and the dynamic development of the clouds. The higher number concentrations in  $N_i$  (but similar values for  $m_i$ ) in both simulations causes difference in the size of the ice crystals and therefore has consequences on the sedimentation velocity of the ice crystals and on the optical properties of the ice clouds. Short wave radiation is scattered more efficiently by smaller ice crystals, which results in optically thicker clouds. In Fig. 9 the difference in the net surface shortwave radiation flux,  $F_{\text{sw}}$ , around noon at the 26 to 29 May and the difference in the net surface long wave radiation flux,  $F_{\text{lw}}$ , around midnight at the 26 to 29 May between simulation *C* and REF is shown as a function of the vertically averaged  $N_d$  at cloud ice containing grid cells in case *C*. During noon, the distribution of the differences in  $F_{\text{sw}}$  show a decrease as a function of  $N_d$  reaching  $-75\text{ W m}^{-2}$  at  $N_d = 100\text{ cm}^{-3}$ . The distribution of differences in  $F_{\text{lw}}$  show a slight increase as a function of  $N_d$ . This can be explained by the less effective sedimentation of the smaller ice crystals which can cause a slight increase in the ice water path.

## Saharan dust event impacts on cloud formation over Western Europe

M. Bangert et al.

Title Page

Abstract

Introduction

Conclusions

References

Tables

Figures

⏪

⏩

◀

▶

Back

Close

Full Screen / Esc

Printer-friendly Version

Interactive Discussion



**Saharan dust event impacts on cloud formation over Western Europe**

M. Bangert et al.

[Title Page](#)[Abstract](#)[Introduction](#)[Conclusions](#)[References](#)[Tables](#)[Figures](#)[⏪](#)[⏩](#)[◀](#)[▶](#)[Back](#)[Close](#)[Full Screen / Esc](#)[Printer-friendly Version](#)[Interactive Discussion](#)

The temporal evolution of the median effective radii of cloud droplets,  $r_c$ , and ice crystals,  $r_i$ , calculated for domain  $D1$ , in simulation  $C$  and REF is shown in Fig. 10. For  $r_c$  slightly lower values occur in case  $C$  with maximum differences to case REF mostly lower than  $1\ \mu\text{m}$ . In contrast,  $r_i$  is significantly lower in simulation  $C$  on the order of 10–25  $\mu\text{m}$ . The difference in  $r_i$  scales with the time evolution of the magnitude of  $r_i$ . Small  $r_i$  indicate that ice clouds occur mainly at greater heights, where the difference in  $r_i$  is much smaller due to the controlling influence of homogeneous freezing.

Figure 11 shows the temporal evolution of domain averaged cloud properties and radiation fluxes in simulation  $C$  and REF. The temporal evolution of averaged vertical integrated cloud water content, LWP, and ice water content, IWP, shows values of similar magnitude in simulation  $C$  and REF with positive and negative difference of a few percent. Whereas LWP shows most of the time slightly lower values and IWP slightly higher values in case  $C$ . Differences in LWP and IWP are mainly caused by differences in the dynamics of the cloud systems. The average in-cloud vertical velocity,  $w_{\text{cloud}}$ , shows slightly higher values in case  $C$  during the first three days of the dust event. This can be explained by more effective glaciation of mixed phase clouds in case  $C$  and the additional release of latent heat. On the last day  $w_{\text{cloud}}$  is lower in simulation  $C$  which is also reflected in a lower LWP. In general, differences in dynamics can be driven by different processes, e.g. changes in radiation and consequently temperature caused by modified cloud properties, and are hard to relate directly with a specific individual process.

In both simulations, the average hourly precipitation rate, PR is almost identical. Difference in PR scale mostly with the differences in LWP and IWP, e.g. during the last two days of the dust event were the largest differences occur. Despite the almost identical PR, the local differences can be large due to spatial shifts in the distribution of precipitation.

The domain average  $F_{\text{sw}}$  shows systematic differences between simulation  $C$  and REF with lower values in simulation  $C$ . The maximum  $F_{\text{sw}}$  is reduced significantly in case  $C$  by 10 to 20  $\text{W m}^{-2}$ . The largest difference in  $F_{\text{sw}}$  occurs on 27 May with

20  $W m^{-2}$  lower values in case *C*. During this day the dust amount is highest in the model domain. Because LWP and IWP are almost identical in both simulations, the difference in  $F_{sw}$  can be directly related to the impact of the dust particles on the radiative properties of the ice clouds in case *C* (Fig. 9). The temporal evolution of the average  
5  $F_{lw}$  shows just small differences between simulation *C* and REF with a maximum of  $+1.5 W m^{-2}$ .

The difference in the net radiation fluxes at the surface have an impact on the simulated temperatures. The domain averaged daily temperature maximum of the temperature in a height of 2 m above ground,  $T_{2m}$  is up to 0.3 K lower in case *C* than in  
10 case REF.  $T_{2m}$  is lower in case *C* until the daily temperature minimum is reached in the early morning, where  $T_{2m}$  in both simulations converge again. Despite the small difference in the domain average  $T_{2m}$ , the differences are locally much larger. This will be discussed in Sect. 4.5.

#### 4.4 Direct dust impact on radiation

15 Until now we investigated only the impact of dust on the atmospheric state due to the interaction of dust particles with cloud microphysical and optical properties. During the dust event the dust particles interact also directly with the radiation fields of the atmosphere due to scattering and absorption of short and longwave radiation. Results of simulation CR, which includes additionally to the interaction with the clouds also the  
20 direct interaction of dust particles with radiation, are shown together with the results of simulation *C* and REF in Fig. 11. The domain averaged dust optical depth at a wavelength of 550 nm,  $\tau_{dust}$ , increases during the dust event up to 0.36 at the 27 May. During the last two days of the dust event  $\tau_{dust}$  decreases again to 0.1. The direct interaction of the dust particles with radiation causes lower values of  $F_{sw}$  of up to  $-80 W m^{-2}$  in  
25 maximum at 27 May in case CR in comparison to case REF. On the other days of the dust event the maximum  $F_{sw}$  is 40 to  $60 W m^{-2}$  lower in case CR with respect to case REF. Due to the interaction of the dust particles with the long wave radiation fields  $F_{lw}$

### Saharan dust event impacts on cloud formation over Western Europe

M. Bangert et al.

Title Page

Abstract

Introduction

Conclusions

References

Tables

Figures



Back

Close

Full Screen / Esc

Printer-friendly Version

Interactive Discussion



is in the order of 3 to 10 W m<sup>-2</sup> higher in case CR in comparison to the cases *C* and REF.

The direct impact of the dust particles in simulation CR causes lower daily maxima of  $T_{2m}$  when compared to simulation *C*. The domain averaged  $T_{2m}$  is 0.5 K lower in CR in comparison to REF at the 27 May. During the night  $T_{2m}$  converge in the different simulations and get even slightly higher values of  $T_{2m}$  in case CR in comparison to *C* due to the higher values of  $F_{lw}$ . The additional temperature decrease during the day in CR in comparison to *C* (from the direct radiative forcing of dust) is comparable in magnitude to the decrease in *C* in comparison to REF (by the interaction of dust with the cloud properties alone). Whether the direct impact on the radiation or the interaction with the clouds has the larger impact on the domain averaged  $T_{2m}$  varies from day to day depending on e.g. the spatial distribution of clouds and dust particles.

#### 4.5 Impact on $T_{2m}$

In Fig. 12 the impact of the dust on average  $T_{2m}$  is depicted for interaction with cloud properties only (*C* minus REF) and for direct interaction with radiation together with the interaction with cloud properties (CR minus REF) for the whole model domain. The  $T_{2m}$  for case *C* at noon is systematically lower over the continent by -0.2 to -1 K. Isolated areas where  $T_{2m}$  in case *C* is higher than in case REF can be attributed to small spatial and temporal differences in the distribution of the clouds. The difference in  $T_{2m}$  at midnight is lower in comparison to noon time. The  $T_{2m}$  at midnight in case *C* is lower by -0.1 to -0.4 K over the continent. The maximum difference is in the eastern part of France. On average over the whole dust event (26–29 May)  $T_{2m}$  in case *C* is systematically lower than in case REF by -0.2 to -0.5 K over the continent. The maximum differences in  $T_{2m}$  are in the areas of the maximum average dust concentrations (Fig. 4).

The average difference in  $T_{2m}$  from combined interaction of dust with clouds and radiation (difference between simulation CR and REF) shows negative values during

### Saharan dust event impacts on cloud formation over Western Europe

M. Bangert et al.

Title Page

Abstract

Introduction

Conclusions

References

Tables

Figures



Back

Close

Full Screen / Esc

Printer-friendly Version

Interactive Discussion



noon time of up to  $-1.8\text{ K}$  in the areas of the maximum dust concentrations. During midnight, the average difference in  $T_{2\text{m}}$  is only negative in the areas with a high negative difference during daytime. In all other areas the difference is slightly positive with values up to  $+1\text{ K}$  locally. The average difference in  $T_{2\text{m}}$  between the simulations CR and REF calculated for the whole period of the dust event shows systematically negative values in the order of  $-0.2\text{ K}$  for the whole continent with maxima up to  $-1\text{ K}$  locally.

As mentioned before, an analysis of the weather forecast results for SW-Germany showed too high  $T_{2\text{m}}$  (by up to  $+2\text{ K}$ ) in comparison with station observations in the afternoon during the dust event. In the early morning hours, the predicted  $T_{2\text{m}}$  converged with the observations. In Fig. 12 the temporal evolution of the simulated  $T_{2\text{m}}$  averaged over an area including SW-Germany,  $\Omega$ , is shown for REF, C, and CR. The difference between CR and REF reaches up to  $-1\text{ K}$  at the afternoon. In the early morning hours  $T_{2\text{m}}$  in CR and REF converge again. Comparing  $T_{2\text{m}}$  in CR and C shows that in this case the impact of dust on  $T_{2\text{m}}$  was dominated by the interaction of dust with clouds at the 26 May and 29 May and by the direct interaction of dust with radiation at the 27 May and 28 May.

This simulation results indicate that the bias in the operational weather forecast can be attributed to the missing interaction of the dust particles with clouds and radiation. Although the observed bias of  $T_{2\text{m}}$  in the weather forecast is two times larger than the simulated difference in  $T_{2\text{m}}$  the temporal evolution is identical. The differences in the magnitude can be explained by uncertainties in the cloud cover and in the exact position of the dust plume; e.g. the differences in  $T_{2\text{m}}$  in Eastern France reach magnitudes comparable to the observed bias.

Both processes (the interaction with clouds and the direct interaction with the radiation) contribute in a similar magnitude to the simulated differences in  $T_{2\text{m}}$ . Whether the direct impact on the radiation or the interaction with the clouds has the bigger impact on  $T_{2\text{m}}$  varies depending on e.g. the spatial distribution of clouds and dust particles.

## Saharan dust event impacts on cloud formation over Western Europe

M. Bangert et al.

[Title Page](#)[Abstract](#)[Introduction](#)[Conclusions](#)[References](#)[Tables](#)[Figures](#)[⏪](#)[⏩](#)[◀](#)[▶](#)[Back](#)[Close](#)[Full Screen / Esc](#)[Printer-friendly Version](#)[Interactive Discussion](#)

## 5 Conclusions

We investigated the impact of mineral dust particles on clouds, radiation, and atmospheric state during a strong Saharan dust event over Europe in May 2008, applying a comprehensive online-coupled regional model framework that explicitly treats particle microphysics and chemical composition. Sophisticated parameterizations for aerosol activation and ice nucleation, together with two-moment cloud microphysics are used to calculate the interaction of the different particles with clouds depending on their physical and chemical properties.

It is shown that the model framework is able to reproduce the measured aerosol mass concentrations during the dust event reasonably well and capture the aerosol background before the arrival of the dust, as well as the spatial distributions of the clouds in comparison with satellite measurements. Dust particles act as CCN and IN in the atmosphere and can interact with clouds in several ways depending on the atmospheric conditions and cloud type.

For temperatures lower than the level of homogeneous freezing the dust particles have to compete with the homogeneous freezing of liquid aerosol particles for water vapor during the ice nucleation. Though the concentration of frozen dust particles is up to  $100\text{ l}^{-1}$  during the ice nucleation events we found no significant impact on the number and mass concentration of ice crystals in this temperature range.

The impact of the dust on cloud droplet number concentration was found to be low, with just a slight increase in cloud droplet number concentration for both uncoated and coated dust. The number of activated dust particles was found to be in the order of 1 to  $20\text{ cm}^{-3}$ , with higher numbers in the case of the coated dust particles. The additional activation of dust particles caused lower maximum supersaturations during the activation process, especially in the case of the coated dust particles.

Mineral dust particles are found to have the largest impact on clouds in a temperature range between freezing level and the level of homogeneous freezing, where they determine the number concentration of ice crystals due to efficient heterogeneous freezing of the dust particles and modify the glaciation of mixed phase clouds. Our simulations

### Saharan dust event impacts on cloud formation over Western Europe

M. Bangert et al.

Title Page

Abstract

Introduction

Conclusions

References

Tables

Figures



Back

Close

Full Screen / Esc

Printer-friendly Version

Interactive Discussion



## Saharan dust event impacts on cloud formation over Western Europe

M. Bangert et al.

Title Page

Abstract

Introduction

Conclusions

References

Tables

Figures



Back

Close

Full Screen / Esc

Printer-friendly Version

Interactive Discussion



show that during the dust events ice crystals concentrations were increased twofold in this temperature range in comparison to a reference simulations which neglects the interaction of the dust with the atmosphere. As a consequence the liquid water fraction was reduced significantly with 60 % less grid points containing cloud water in the temperature range between 263 K to 235 K.

The strong increase in ice crystal number concentration has an influence on the optical properties of the ice clouds during the time of the dust event due to a significant decrease of effective radii of the ice crystals in the order of up to  $-25\ \mu\text{m}$  on average. It was shown that depending on the number concentration of dust available for ice nucleation the incoming short-wave radiation at the surface was reduced up to  $-75\ \text{W m}^{-2}$  at  $N_d = 100\ \text{cm}^{-3}$ . Consequently, a reduction in surface temperature in the order of up to 1 K over Europe during the day time arises from aerosol-cloud interactions. In the morning hours, the surface temperatures converge again between the different simulations. On average over the whole period of the dust event a reduction in surface temperature in the order of  $-0.2\ \text{K}$  to  $-0.4\ \text{K}$  was found in the eastern part of France and Western Germany.

The simulated aerosol optical thickness of the dust particles was found to be in the order of 0.2 to 0.5 on average during the dust event over Europe. This caused an additional reduction in the incoming short-wave radiation which was found to be in the order of  $-80\ \text{W m}^{-2}$  on 27 May. On the other days of the event the reduction was found to be in the order of  $-40$  to  $-60\ \text{W m}^{-2}$ . In contrast to the aerosol-cloud interaction only, the incoming long-wave radiation at the surface was increased significantly in the order of  $+10\ \text{W m}^{-2}$ .

The direct impact on radiation together with the impact on the clouds caused lower surface temperatures of up to  $-1.8\ \text{K}$  in the areas of the maximum dust concentrations during the daytime. Due to the enhanced incoming long-wave radiation a temperatures increase was found for most parts of Europe during the night time. Only in the areas with the maximum temperature difference during the day the night temperatures were still below the ones simulated neglecting the interaction of dust with the atmosphere.

## Saharan dust event impacts on cloud formation over Western Europe

M. Bangert et al.

Title Page

Abstract

Introduction

Conclusions

References

Tables

Figures

⏪

⏩

◀

▶

Back

Close

Full Screen / Esc

Printer-friendly Version

Interactive Discussion



On average the overall impact of the dust caused a reduction in surface temperature in the order of  $-0.2$  to  $-0.5$  K for most parts of France, Germany, and Italy during the dust event. The maximum difference in surface temperature was found in the East of France, the Benelux, and Western Germany with up to  $-1$  K.

The simulations suggest that the bias which was found in numerical weather forecast during the period of the dust event can be explained by the missing aerosol cloud interaction in current weather forecast simulations. Weather forecast models use climatological aerosol conditions to represent AOT and calculate ice crystal and clouds droplet number concentrations. Hence they are not able to represent conditions which differ significantly from the climatological values, which is the case during strong dust events over Europe.

*Acknowledgements.* We thank H. Flentje (DWD) for providing the  $PM_{10}$  measurement data and U. Damrath (DWD) for providing the forecast validation information. We gratefully acknowledge A. Seifert (DWD) for his support with his cloud microphysic scheme, E. Zuber (ETH) for providing the code for the improved parametrization of cloud optical properties, and R. Frey (UW-Madison) for his information on the MODIS cloud product. This work was supported by the Karlsruhe House of Young Scientist (KHYS). AN, DB, VK and PK acknowledge support from an NSF CAREER award, and grants from NASA MAP, NASA ACP and NOAA OGP.

## References

- Baldauf, M., Seifert, A., Förstner, J., Majewski, D., Raschendorfer, M., and Reinhardt, T.: Operational convective-scale numerical weather prediction with the COSMO model: description and sensitivities, *Mon. Weather Rev.*, 139, 3887–3905, doi:10.1175/MWR-D-10-05013.1, e-View, 2011. 31941, 31942
- Bangert, M., Kottmeier, C., Vogel, B., and Vogel, H.: Regional scale effects of the aerosol cloud interaction simulated with an online coupled comprehensive chemistry model, *Atmos. Chem. Phys.*, 11, 4411–4423, doi:10.5194/acp-11-4411-2011, 2011. 31943, 31946
- Barahona, D. and Nenes, A.: Parameterization of cirrus cloud formation in large-

## Saharan dust event impacts on cloud formation over Western Europe

M. Bangert et al.

Title Page

Abstract

Introduction

Conclusions

References

Tables

Figures

⏪

⏩

◀

▶

Back

Close

Full Screen / Esc

Printer-friendly Version

Interactive Discussion

scale models: homogeneous nucleation, *J. Geophys. Res.-Atmos.*, 113, D11211, doi:10.1029/2007JD009355, 2008. 31946, 31947

Barahona, D. and Nenes, A.: Parameterizing the competition between homogeneous and heterogeneous freezing in cirrus cloud formation – monodisperse ice nuclei, *Atmos. Chem. Phys.*, 9, 369–381, doi:10.5194/acp-9-369-2009, 2009a. 31946, 31947, 31955

Barahona, D. and Nenes, A.: Parameterizing the competition between homogeneous and heterogeneous freezing in ice cloud formation – polydisperse ice nuclei, *Atmos. Chem. Phys.*, 9, 5933–5948, doi:10.5194/acp-9-5933-2009, 2009b. 31942, 31946

Barahona, D., West, R. E. L., Stier, P., Romakkaniemi, S., Kokkola, H., and Nenes, A.: Comprehensively accounting for the effect of giant CCN in cloud activation parameterizations, *Atmos. Chem. Phys.*, 10, 2467–2473, doi:10.5194/acp-10-2467-2010, 2010a. 31942, 31945, 31946

Barahona, D., Rodriguez, J., and Nenes, A.: Sensitivity of the global distribution of cirrus ice crystal concentration to heterogeneous freezing, *J. Geophys. Res.-Atmos.*, 115, D23213, doi:10.1029/2010JD014273, 2010b. 31940

Blahak, U.: Towards a Better Representation of High Density Ice Particles in a State-of-the-Art Two-Moment Bulk Microphysical Scheme, Extended Abstract, International Conference on Clouds and Precipitation, Cancun, 7–11 July 2008, available at: [http://cabernet.atmosfcu.unam.mx/ICCP-2008/abstracts/Program\\_on\\_line/Poster\\_07/Blahak\\_extended\\_1.pdf](http://cabernet.atmosfcu.unam.mx/ICCP-2008/abstracts/Program_on_line/Poster_07/Blahak_extended_1.pdf) (last access: 30 November 2011), 2008. 31943

Cantrell, W. and Heymsfield, A.: Production of ice in tropospheric clouds – a review, *B. A. M. Meteorol. Soc.*, 86, 795–807, doi:10.1175/BAMS-86-6-795, 2005. 31940

Cavazos, C., Todd, M. C., and Schepanski, K.: Numerical model simulation of the Saharan dust event of 6–11 March 2006 using the Regional Climate Model version 3 (RegCM3), *J. Geophys. Res.-Atmos.*, 114, D12109, doi:10.1029/2008JD011078, 2009. 31939

Chaboureaud, J.-P., Richard, E., Pinty, J.-P., Flamant, C., Di Girolamo, P., Kiemle, C., Behrendt, A., Chepfer, H., Chiriaco, M., and Wulfmeyer, V.: Long-range transport of Saharan dust and its radiative impact on precipitation forecast: a case study during the convective and Orographically-induced Precipitation Study (COPS), *Q. J. Roy. Meteor. Soc.*, 137, 236–251, doi:10.1002/qj.719, 2011. 31939

Doms, G., Förstner, J., Heise, E., Herzog, H.-J., and Raschendorfer, M.: Nonhydrostatic Regional Model LM, Part II: Physical Parameterization, Tech. Rep., Deutscher Wetterdienst, Offenbach, 2005. 31943

Edwards, J. M., Havemann, S., Thelen, J.-C., and Baran, A. J.: A new parametrization for the

**Saharan dust event  
impacts on cloud  
formation over  
Western Europe**

M. Bangert et al.

[Title Page](#)[Abstract](#)[Introduction](#)[Conclusions](#)[References](#)[Tables](#)[Figures](#)[⏪](#)[⏩](#)[◀](#)[▶](#)[Back](#)[Close](#)[Full Screen / Esc](#)[Printer-friendly Version](#)[Interactive Discussion](#)

radiative properties of ice crystals: comparison with existing schemes and impact in a GCM, Atmos. Res., 83, 19–35, doi:10.1016/j.atmosres.2006.03.002, 2007. 31948

Emmons, L. K., Walters, S., Hess, P. G., Lamarque, J.-F., Pfister, G. G., Fillmore, D., Granier, C., Guenther, A., Kinnison, D., Laepple, T., Orlando, J., Tie, X., Tyndall, G., Wiedinmyer, C.,  
5 Baughcum, S. L., and Kloster, S.: Description and evaluation of the Model for Ozone and Related chemical Tracers, version 4 (MOZART-4), Geosci. Model Dev., 3, 43–67, doi:10.5194/gmd-3-43-2010, 2010. 31949

Field, P. R., Möhler, O., Connolly, P., Krämer, M., Cotton, R., Heymsfield, A. J., Saathoff, H.,  
and Schnaiter, M.: Some ice nucleation characteristics of Asian and Saharan desert dust,  
10 Atmos. Chem. Phys., 6, 2991–3006, doi:10.5194/acp-6-2991-2006, 2006. 31940, 31953

Hoose, C., Lohmann, U., Erdin, R., and Tegen, I.: The global influence of dust mineralogical  
composition on heterogeneous ice nucleation in mixed-phase clouds, Environ. Res. Lett., 3,  
025003, doi:10.1088/1748-9326/3/2/025003, 2008. 31940

Hu, Y. X. and Stamnes, K.: An accurate parameterization of the radiative properties of water  
clouds suitable for use in climate models, J. Climate, 6, 728–742, 1993. 31948

Karydis, V., Kumar, P., Barahona, D., and Nenes, A.: On the effect of insoluble dust particles  
on global CCN and droplet number, J. Geophys. Res., doi:10.1029/2011JD016283, in press,  
2011. 31941

Klein, H., Nickovic, S., Haunold, W., Bundke, U., Nillius, B., Ebert, M., Weinbruch, S.,  
20 Schuetz, L., Levin, Z., Barrie, L. A., and Bingemer, H.: Saharan dust and ice nuclei over  
Central Europe, Atmos. Chem. Phys., 10, 10211–10221, doi:10.5194/acp-10-10211-2010,  
2010. 31941

Koop, T., Luo, B. P., Tsias, A., and Peter, T.: Water activity as the determinant for homogeneous  
ice nucleation in aqueous solutions, Nature, 406, 611–614, 2000. 31946

25 Kumar, P., Sokolik, I. N., and Nenes, A.: Parameterization of cloud droplet formation for global  
and regional models: including adsorption activation from insoluble CCN, Atmos. Chem.  
Phys., 9, 2517–2532, doi:10.5194/acp-9-2517-2009, 2009. 31942, 31945, 31954

Kumar, P., Sokolik, I. N., and Nenes, A.: Measurements of cloud condensation nuclei activity  
and droplet activation kinetics of fresh unprocessed regional dust samples and minerals,  
30 Atmos. Chem. Phys., 11, 3527–3541, doi:10.5194/acp-11-3527-2011, 2011. 31941, 31945,  
31950

Levin, Z., Ganor, E., and Gladstein, V.: The effects of desert particles coated with sulfate on  
rain formation in the Eastern Mediterranean, J. Appl. Meteorol., 35, 1511–1523, 1996. 31941

## Saharan dust event impacts on cloud formation over Western Europe

M. Bangert et al.

Title Page

Abstract

Introduction

Conclusions

References

Tables

Figures

⏪

⏩

◀

▶

Back

Close

Full Screen / Esc

Printer-friendly Version

Interactive Discussion



- Lohmann, U. and Diehl, K.: Sensitivity studies of the importance of dust ice nuclei for the indirect aerosol effect on stratiform mixed-phase clouds, *J. Atmos. Sci.*, 63, 968–982, 2006. 31940
- Lowell, S., Shields, J. E., Thomas, M. A., and Thommes, M.: Characterization of porous solids and powders: surface area, pore size and density, in: *Particle Technology Series*, vol. 16, Kluwer Academic Publishers, Dordrecht, 2004. 31945
- Lundgren, K.: *Direct Radiative Effects of Sea Salt on the Regional Scale*, Ph.D. thesis, Karlsruhe Institute of Technology, Karlsruhe, 2010. 31943, 31948
- Menzel, W. P., Frey, R. A., Zhang, H., Wylie, D. P., Moeller, C. C., Holz, R. E., Maddux, B., Baum, B. A., Strabala, K. I., and Gumley, L. E.: MODIS global cloud-top pressure and amount estimation: algorithm description and results, *J. Appl. Meteorol. Clim.*, 47, 1175–1198, doi:10.1175/2007JAMC1705.1, 2008. 31951
- Min, Q. and Li, R.: Longwave indirect effect of mineral dusts on ice clouds, *Atmos. Chem. Phys.*, 10, 7753–7761, doi:10.5194/acp-10-7753-2010, 2010. 31940
- Min, Q.-L., Li, R., Lin, B., Joseph, E., Wang, S., Hu, Y., Morris, V., and Chang, F.: Evidence of mineral dust altering cloud microphysics and precipitation, *Atmos. Chem. Phys.*, 9, 3223–3231, doi:10.5194/acp-9-3223-2009, 2009. 31940
- Möhler, O., Field, P. R., Connolly, P., Benz, S., Saathoff, H., Schnaiter, M., Wagner, R., Cotton, R., Krämer, M., Mangold, A., and Heymsfield, A. J.: Efficiency of the deposition mode ice nucleation on mineral dust particles, *Atmos. Chem. Phys.*, 6, 3007–3021, doi:10.5194/acp-6-3007-2006, 2006. 31940, 31953
- Morales, R. and Nenes, A.: Characteristic updrafts for computing distribution-averaged cloud droplet number, autoconversion rate and effective radius, *J. Geophys. Res.*, 115, D18220, doi:10.1029/2009JD013233, 2010. 31948
- Niemand, M., Möhler, O., Vogel, B., Vogel, H., Hoose, C., Connolly, P., Klein, H., Bingemer, H., DeMott, P., Skrotzki, S., and Leisner, T.: Parameterization of immersion freezing on mineral dust particles: an application in a regional scale model, *J. Atmos. Sci.*, submitted, 2011. 31947
- Noppel, H., Blahak, U., Beheng, K. D., and Seifert, A.: A Two-Moment Cloud Microphysics Scheme with Two Process-Separated Modes of Graupel, 12. AMS Conference on Cloud Physics, 10–14 July 2006, Madison, Wisconsin, available at: <http://ams.confex.com/ams/pdfpapers/113532.pdf> (last access: 30 November 2011), 2006. 31943
- Perez, C., Nickovic, S., Pejanovic, G., Baldasano, J. M., and Oezsoy, E.: Interactive dust-

## Saharan dust event impacts on cloud formation over Western Europe

M. Bangert et al.

[Title Page](#)

[Abstract](#)

[Introduction](#)

[Conclusions](#)

[References](#)

[Tables](#)

[Figures](#)

[⏪](#)

[⏩](#)

[◀](#)

[▶](#)

[Back](#)

[Close](#)

[Full Screen / Esc](#)

[Printer-friendly Version](#)

[Interactive Discussion](#)



radiation modeling: a step to improve weather forecasts, *J. Geophys. Res.-Atmos.*, 111, D16206, doi:10.1029/2005JD006717, 2006. 31939

Phillips, V. T. J., DeMott, P. J., and Andronache, C.: An empirical parameterization of heterogeneous ice nucleation for multiple chemical species of aerosol, *J. Atmos. Sci.*, 65, 2757–2783, doi:10.1175/2007JAS2546.1, 2008. 31947, 31953

Pradelle, F. and Cautenet, G.: Radiative and microphysical interactions between marine stratocumulus clouds and Saharan dust – 2. Modeling, *J. Geophys. Res.-Atmos.*, 107, 4413, doi:10.1029/2000JD000156, 2002. 31940

Pregger, T., Thiruchittampalam, B., and Friedrich, R.: Ermittlung von Emissionsdaten zur Untersuchung der Klimawirksamkeit von Rußpartikeln in Baden-Württemberg, Final report, IER Universität Stuttgart, Stuttgart, 2007. 31950

Riemer, N., Vogel, B., Vogel, H., and Fiedler, F.: Modeling aerosols on the mesoscale: treatment of soot aerosol and its radiative effects, *J. Geophys. Res.*, 108, 4601, doi:10.1029/2003JD003448, 2003. 31942

Ritter, B. and Geleyn, J. F.: A comprehensive radiation scheme for numerical weather prediction models with potential applications in climate simulations, *Mon. Weather Rev.*, 120, 303–325, doi:10.1175/1520-0493(1992)120<0303:ACRSFN>2.0.CO;2, 1992. 31948

Rosenfeld, D., Rudich, Y., and Lahav, R.: Desert dust suppressing precipitation: a possible desertification feedback loop, *Proc. Natl. Acad. Sci.*, 98, 5975–5980, doi:10.1073/pnas.101122798, 2001. 31940

Seifert, A. and Beheng, K. D.: A two-moment cloud microphysics parameterization for mixed-phase clouds. Part 1: Model description, *Meteorol. Atmos. Phys.*, 92, 45–66, doi:10.1007/s00703-005-0112-4, 2006. 31942, 31943, 31944, 31946, 31947

Seifert, A., Khain, A., Pokrovsky, A., and Beheng, K. D.: A comparison of spectral bin and two-moment bulk mixed-phase cloud microphysics, *Atmos. Res.*, 80, 46–66, 2006. 31943

Seifert, P., Ansmann, A., Mattis, I., Wandinger, U., Tesche, M., Engelmann, R., Mueller, D., Perez, C., and Haustein, K.: Saharan dust and heterogeneous ice formation: Eleven years of cloud observations at a Central European EARLINET site, *J. Geophys. Res.*, 115, D20201, doi:10.1029/2009JD013222, 2010. 31940

Seifert, A., Köhler, C., and Beheng, K. D.: Aerosol-cloud-precipitation effects over Germany as simulated by a convective-scale numerical weather prediction model, *Atmos. Chem. Phys. Discuss.*, 11, 20203–20243, doi:10.5194/acpd-11-20203-2011, 2011. 31944

Solomos, S., Kallos, G., Kushta, J., Astitha, M., Tremback, C., Nenes, A., and Levin, Z.: An

integrated modeling study on the effects of mineral dust and sea salt particles on clouds and precipitation, *Atmos. Chem. Phys.*, 11, 873–892, doi:10.5194/acp-11-873-2011, 2011. 31940

5 Sorjamaa, R. and Laaksonen, A.: The effect of H<sub>2</sub>O adsorption on cloud drop activation of insoluble particles: a theoretical framework, *Atmos. Chem. Phys.*, 7, 6175–6180, doi:10.5194/acp-7-6175-2007, 2007. 31945

Stanelle, T., Vogel, B., Vogel, H., Bäumer, D., and Kottmeier, C.: Feedback between dust particles and atmospheric processes over West Africa during dust episodes in March 2006 and June 2007, *Atmos. Chem. Phys.*, 10, 10771–10788, doi:10.5194/acp-10-10771-2010, 2010. 31939, 31943, 31948

10 Sullivan, R. C., Guazzotti, S. A., Sodeman, D. A., and Prather, K. A.: Direct observations of the atmospheric processing of Asian mineral dust, *Atmos. Chem. Phys.*, 7, 1213–1236, doi:10.5194/acp-7-1213-2007, 2007. 31941

Tiedtke, M.: A comprehensive mass flux scheme for cumulus parameterization in large-scale models, *Mon. Weather Rev.*, 117, 1779–1800, 1989. 31944

15 Vogel, B., Vogel, H., Bäumer, D., Bangert, M., Lundgren, K., Rinke, R., and Stanelle, T.: The comprehensive model system COSMO-ART – Radiative impact of aerosol on the state of the atmosphere on the regional scale, *Atmos. Chem. Phys.*, 9, 8661–8680, doi:10.5194/acp-9-8661-2009, 2009. 31943, 31948

20 Waliser, D. E., Li, J. L. F., L'Ecuyer, T. S., and Chen, W. T.: The impact of precipitating ice and snow on the radiation balance in global climate models, *Geophys. Res. Lett.*, 38, L06802, doi:10.1029/2010GL046478, 2011. 31949

Wiacek, A., Peter, T., and Lohmann, U.: The potential influence of Asian and African mineral dust on ice, mixed-phase and liquid water clouds, *Atmos. Chem. Phys.*, 10, 8649–8667, doi:10.5194/acp-10-8649-2010, 2010. 31939

25 Yin, Y. and Chen, L.: The effects of heating by transported dust layers on cloud and precipitation: a numerical study, *Atmos. Chem. Phys.*, 7, 3497–3505, doi:10.5194/acp-7-3497-2007, 2007. 31939

30 Zubler, E. M., Folini, D., Lohmann, U., Lüthi, D., Muhlbauer, A., Pousse-Nottelmann, S., Schär, C., and Wild, M.: Implementation and evaluation of aerosol and cloud microphysics in a regional climate model, *J. Geophys. Res.*, 116, D02211, doi:10.1029/2010JD014572, 2011. 31949

## Saharan dust event impacts on cloud formation over Western Europe

M. Bangert et al.

Title Page

Abstract

Introduction

Conclusions

References

Tables

Figures

⏪

⏩

◀

▶

Back

Close

Full Screen / Esc

Printer-friendly Version

Interactive Discussion



## Saharan dust event impacts on cloud formation over Western Europe

M. Bangert et al.

Title Page

Abstract

Introduction

Conclusions

References

Tables

Figures

◀

▶

◀

▶

Back

Close

Full Screen / Esc

Printer-friendly Version

Interactive Discussion



**Table 1.** Overview of the setup for the nested simulations. The interaction involving aerosol include anthropogenic (if, ic, jf, jc, and s) and sea salt (sa, sb, and sc) modes, whereas dust refers to the dust modes (da, db, and dc) only.

Interactions	REF	C	C*	CR
Cloud–radiation	•	•	•	•
Aerosol–radiation	•	•	•	•
Aerosol–water clouds	•	•	•	•
Aerosol–ice clouds	•	•	•	•
Dust–water clouds (FFH theory)		•		•
Dust–water clouds (Unified theory)			•	
Dust–ice clouds		•	•	•
Dust–radiation				•

## Saharan dust event impacts on cloud formation over Western Europe

M. Bangert et al.

**Table 2.** Overview of the individual aerosol modes, their chemical composition (first block), the involved cloud interaction processes (second block), aerosol dynamical processes (third block), and their initial diameter and standard deviation (fourth block).

	if	ic	jf	jc	s	sa	sb	sc	da	db	dc
Inorg. salts	•	•	•	•		•	•	•			
Organics	•	•	•	•							
Soot		•		•	•						
Dust									•	•	•
Activation (Köhler)	•	•	•	•		•	•	•			
Activation (FFH)					•				•	•	•
Activation (Unified)									•	•	•
Homogeneous freezing	•		•			•	•	•			
Heterogeneous freezing		•		•	•				•	•	•
Coagulation	•	•	•	•	•						
Condensation	•	•	•	•	•						
	Initial diameter in $\mu\text{m}$										
	0.01	0.08	0.07	0.08	0.08	0.2	1	12	1.5	6.7	14.2
	Standard deviation										
	1.7	2	1.7	2	1.4	1.9	2	1.7	1.7	1.6	1.5

[Title Page](#)
[Abstract](#)
[Introduction](#)
[Conclusions](#)
[References](#)
[Tables](#)
[Figures](#)
[⏪](#)
[⏩](#)
[◀](#)
[▶](#)
[Back](#)
[Close](#)
[Full Screen / Esc](#)
[Printer-friendly Version](#)
[Interactive Discussion](#)

**Saharan dust event  
impacts on cloud  
formation over  
Western Europe**

M. Bangert et al.

Title Page

Abstract

Introduction

Conclusions

References

Tables

Figures

◀

▶

◀

▶

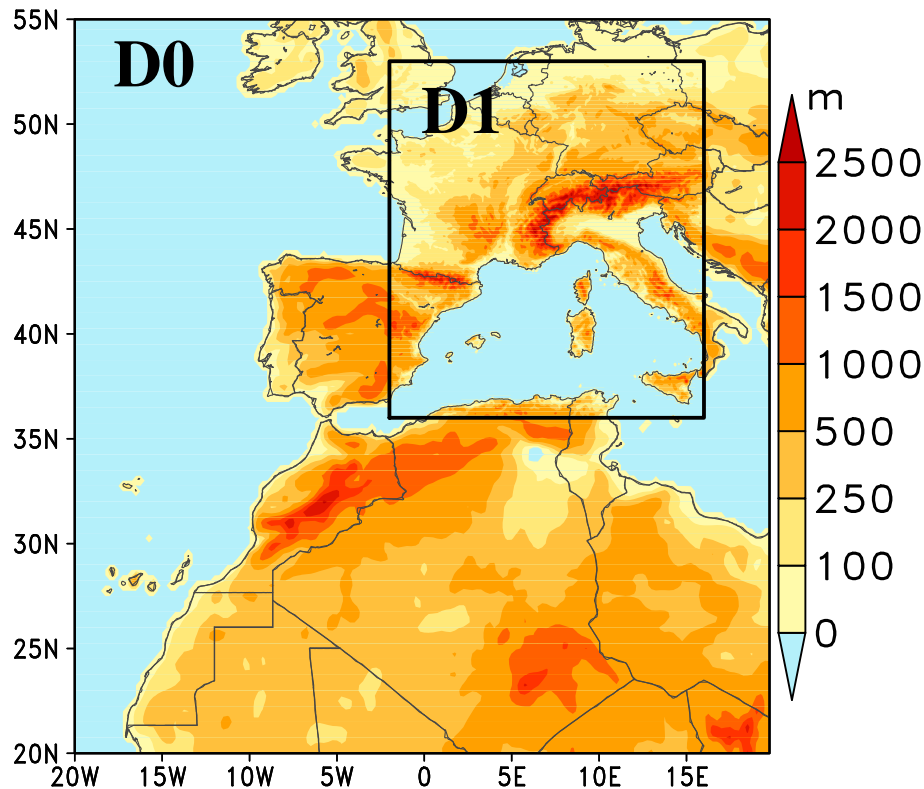
Back

Close

Full Screen / Esc

Printer-friendly Version

Interactive Discussion

**Fig. 1.** Terrain height within the model domains.

**Saharan dust event  
impacts on cloud  
formation over  
Western Europe**

M. Bangert et al.

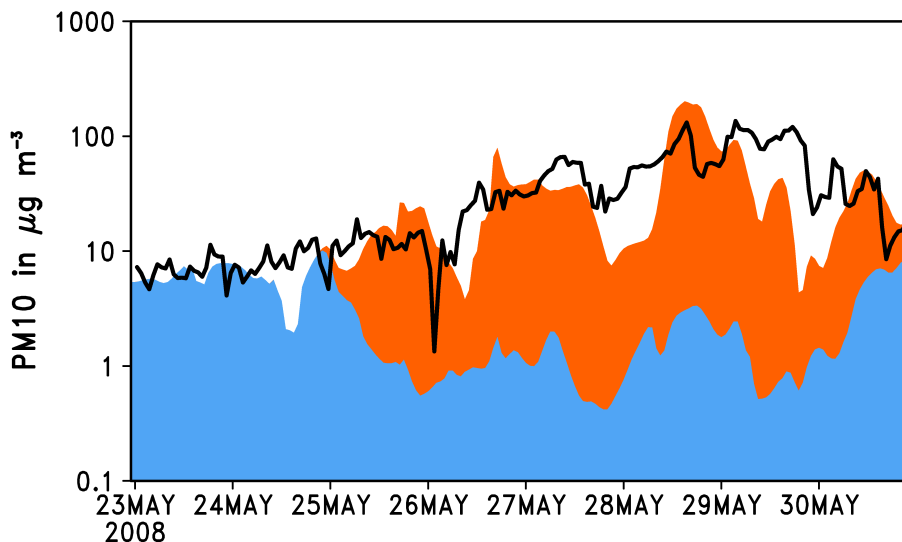


**Fig. 2.** Measured aerosol mass concentration,  $PM_{10}$ , at Hohenpeissenberg (Flentje, 2010, DWD, personal communication) (line) and simulated  $PM_{10}$  (shadings) of the coarse simulation for domain D0. Red shading represents the total aerosol mass concentration of dust particles (mode da and db) and blue shading is the total aerosol mass concentration of all other modes (including anthropogenic aerosol particles and sea salt. Please note that the vertical axis is on  $\log_{10}$ -scale to take the large variation of  $PM_{10}$  during the dust event into account.

**Saharan dust event  
impacts on cloud  
formation over  
Western Europe**

M. Bangert et al.

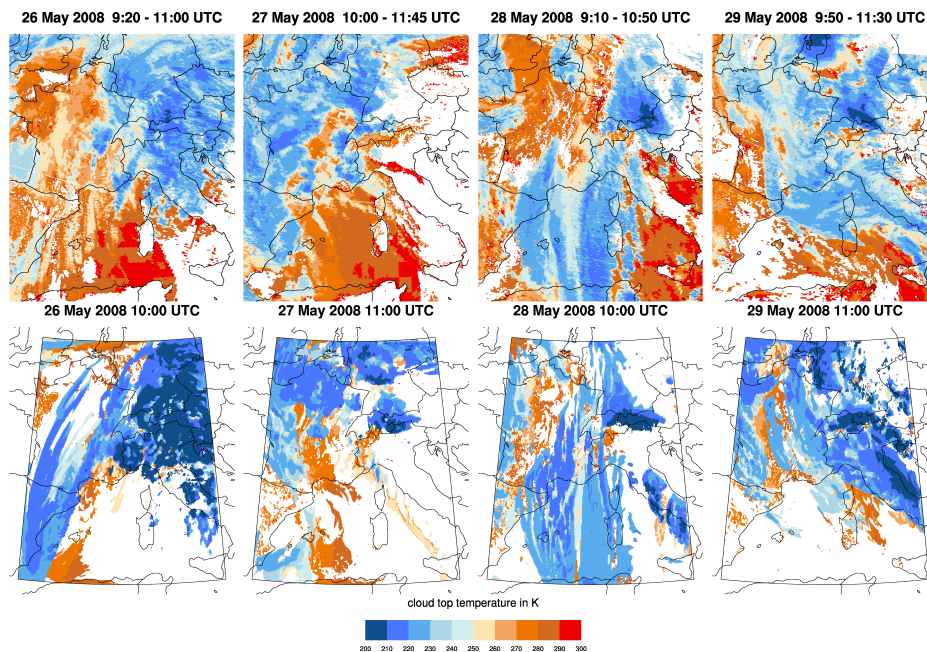


**Fig. 3.** Composites of cloud top temperatures measured with MODIS (top) and simulated cloud top temperature (case C, bottom).

[Title Page](#)[Abstract](#)[Introduction](#)[Conclusions](#)[References](#)[Tables](#)[Figures](#)[⏪](#)[⏩](#)[◀](#)[▶](#)[Back](#)[Close](#)[Full Screen / Esc](#)[Printer-friendly Version](#)[Interactive Discussion](#)

**Saharan dust event impacts on cloud formation over Western Europe**

M. Bangert et al.

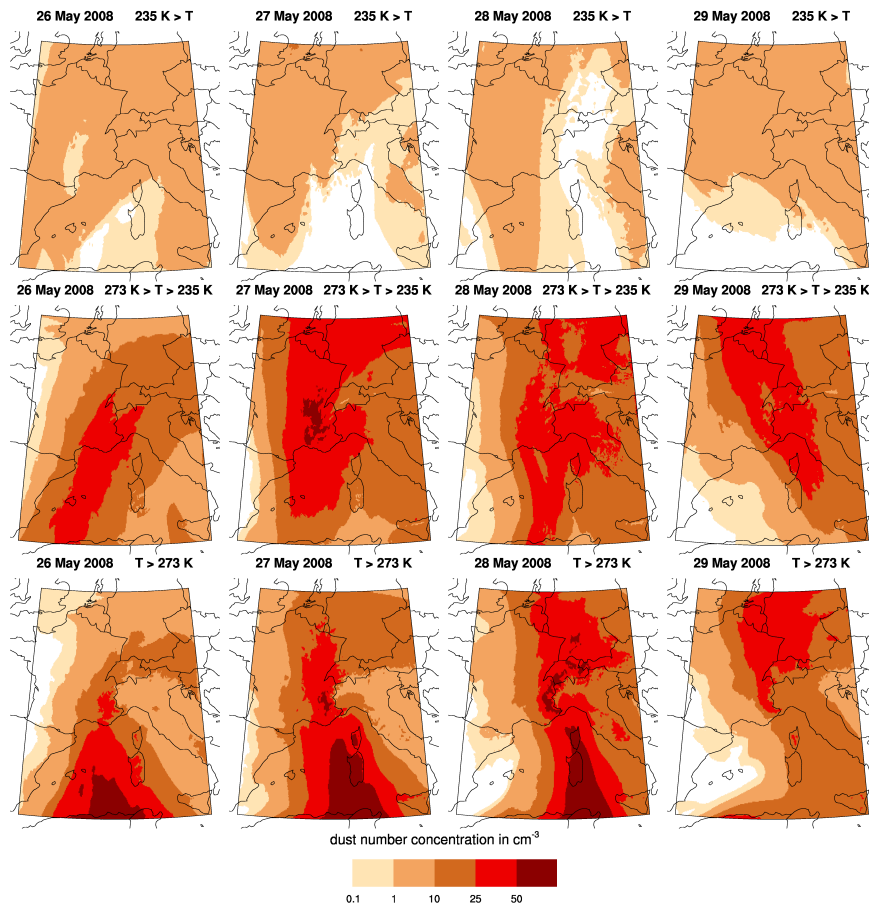


**Fig. 4.** Simulated daily means of dust number concentrations for atmospheric layers below freezing level (bottom), layers favorable of heterogeneous freezing (middle), and layers favorable of homogeneous freezing (top) for 26–29 May 2008.

[Title Page](#)  
[Abstract](#)   [Introduction](#)  
[Conclusions](#)   [References](#)  
[Tables](#)   [Figures](#)  
◀   ▶  
◀   ▶  
[Back](#)   [Close](#)  
[Full Screen / Esc](#)  
[Printer-friendly Version](#)  
[Interactive Discussion](#)



## Saharan dust event impacts on cloud formation over Western Europe

M. Bangert et al.

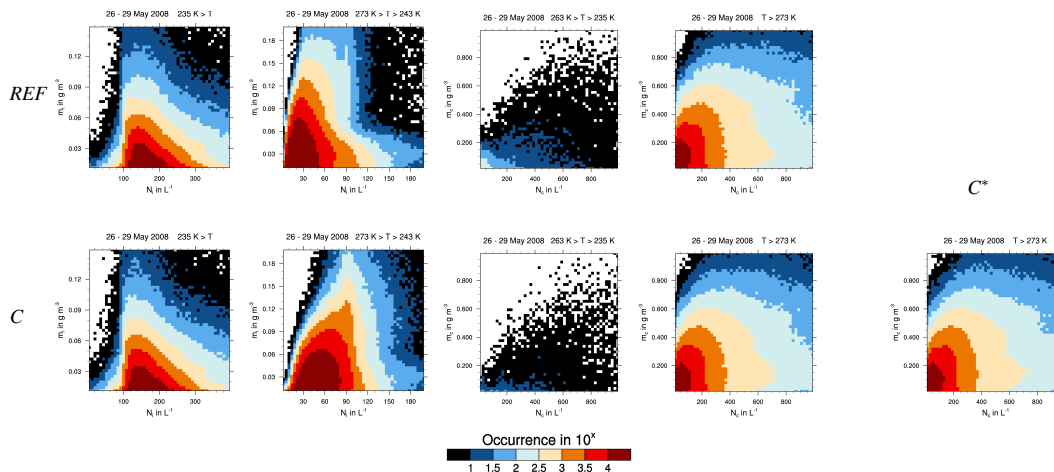


**Fig. 5.** Domain wide joint histogram of number and mass concentrations for cloud droplet and ice crystals calculated for grid points with  $N_d \geq 1 \text{ cm}^{-3}$  and different temperatures ranges for 26–29 May 2008.

Title Page

Abstract

Introduction

Conclusions

References

Tables

Figures

◀

▶

◀

▶

Back

Close

Full Screen / Esc

Printer-friendly Version

Interactive Discussion

## Saharan dust event impacts on cloud formation over Western Europe

M. Bangert et al.

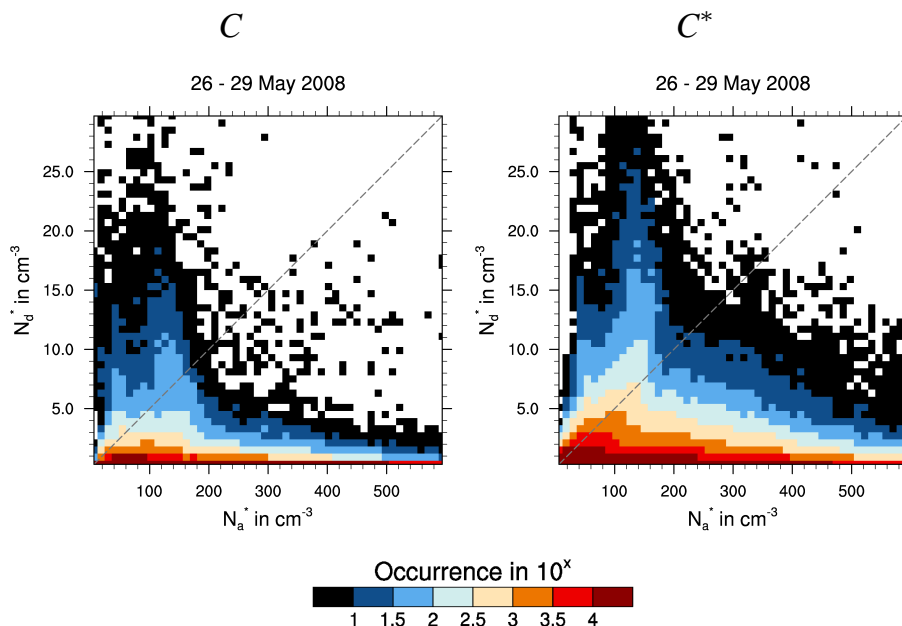


**Fig. 6.** Domain wide joint histogram of activated dust particles,  $N_d^*$ , and total number of activated aerosol particles,  $N_a^*$ , calculated for grid points with  $N_d \geq 1 \text{ cm}^{-3}$  for 26–29 May 2008.

Title Page

Abstract

Introduction

Conclusions

References

Tables

Figures

⏪

⏩

◀

▶

Back

Close

Full Screen / Esc

Printer-friendly Version

Interactive Discussion

## Saharan dust event impacts on cloud formation over Western Europe

M. Bangert et al.

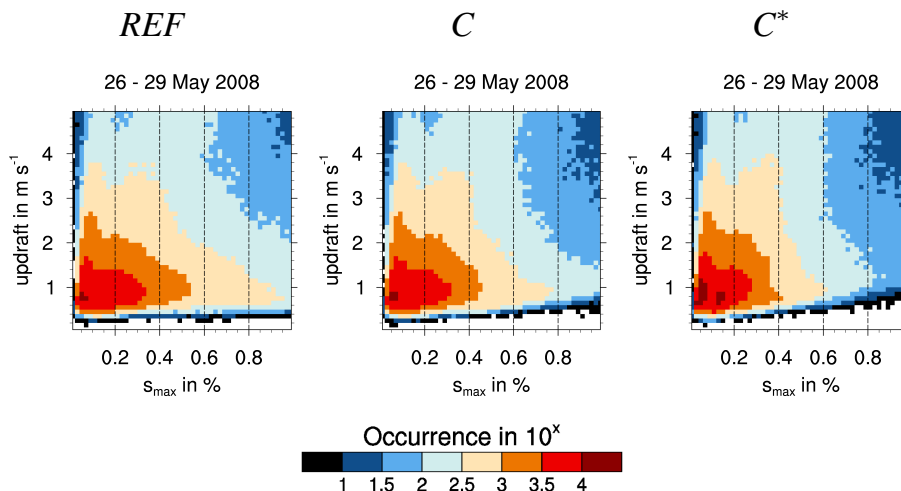


**Fig. 7.** Joint histogram of updraft and maximum supersaturation,  $s_{\text{max}}$ , during activation of particles calculated for grid points with  $N_d \geq 20 \text{ cm}^{-3}$ . The updraft is calculated as  $w + \sqrt{TKE}$ .  $s_{\text{max}}$  is the average of the corresponding updraft PDF (see Eq. (8)).

Title Page

Abstract

Introduction

Conclusions

References

Tables

Figures

◀

▶

◀

▶

Back

Close

Full Screen / Esc

Printer-friendly Version

Interactive Discussion

## Saharan dust event impacts on cloud formation over Western Europe

M. Bangert et al.

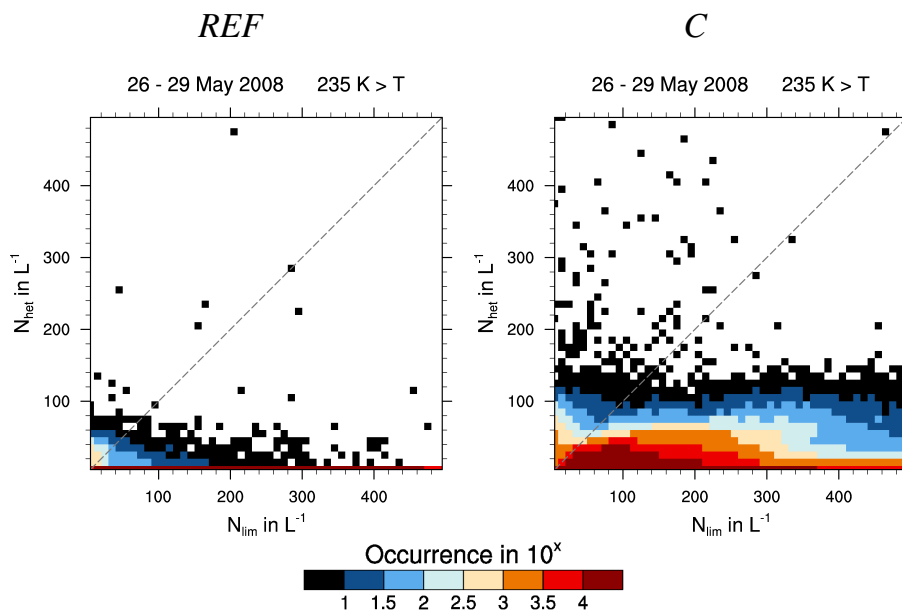


**Fig. 8.** Joint histogram of heterogeneously nucleated ice crystals and  $N_{lim}$ , calculated for grid points with  $N_d \geq 0.1 \text{ cm}^{-3}$ . The dashed line highlights the limit between combined heterogeneous-homogeneous freezing (below the line) and pure heterogeneous freezing only (above the line).

Title Page

Abstract

Introduction

Conclusions

References

Tables

Figures

⏪

⏩

◀

▶

Back

Close

Full Screen / Esc

Printer-friendly Version

Interactive Discussion

## Saharan dust event impacts on cloud formation over Western Europe

M. Bangert et al.

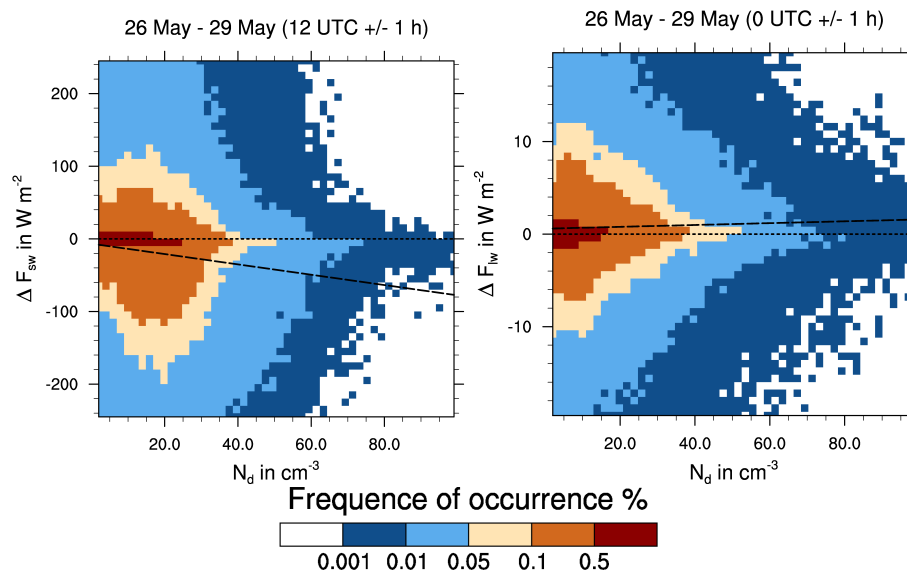


**Fig. 9.** Joint PDFs of differences ( $C$  minus REF) in surface net shortwave radiation flux around noon (left) and in surface net longwave radiation flux around midnight (right) together with average dust concentration at grid points containing cloud ice ( $C$ ). The dashed line is the result of a linear regression fit of the data.

Title Page

Abstract

Introduction

Conclusions

References

Tables

Figures

◀

▶

◀

▶

Back

Close

Full Screen / Esc

Printer-friendly Version

Interactive Discussion

**Saharan dust event  
impacts on cloud  
formation over  
Western Europe**

M. Bangert et al.

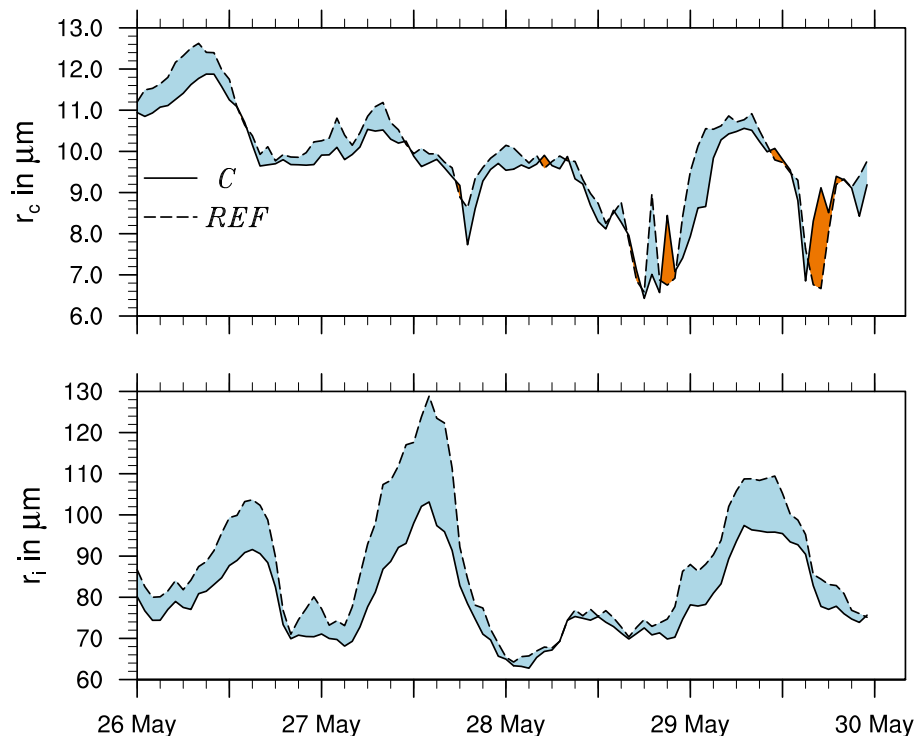


**Fig. 10.** Time series of the average effective radii of cloud droplets  $r_c$  and ice crystal  $r_i$  of domain D1. Solid lines are results from simulation *C* and dashed lines are results from simulation *REF*.  $r_c$  is calculated for gridpoints with a cloud water mass mixing ratio greater than  $0.05 \text{ g kg}^{-1}$  and  $r_i$  for ice crystal mass mixing ratios of more than  $0.001 \text{ g kg}^{-1}$ .

[Title Page](#)[Abstract](#)[Introduction](#)[Conclusions](#)[References](#)[Tables](#)[Figures](#)[◀](#)[▶](#)[◀](#)[▶](#)[Back](#)[Close](#)[Full Screen / Esc](#)[Printer-friendly Version](#)[Interactive Discussion](#)

## Saharan dust event impacts on cloud formation over Western Europe

M. Bangert et al.

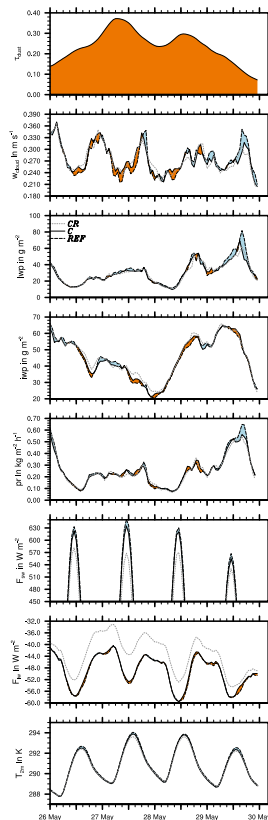


**Fig. 11.** Time series of dust optical thickness ( $\tau_{\text{dust}}$ ), cloud properties ( $w_{\text{cloud}}$ , LWP, and IWP), precipitation rate (PR), net surface radiation fluxes ( $F_{\text{sw}}$  and  $F_{\text{w}}$ ), and temperature ( $T_{2\text{m}}$ ) averaged for domain D1. Solid lines are results from simulation C, dashed lines are results from simulation REF, and dotted gray lines are results from simulation CR.

[Title Page](#)
[Abstract](#)
[Introduction](#)
[Conclusions](#)
[References](#)
[Tables](#)
[Figures](#)
[◀](#)
[▶](#)
[◀](#)
[▶](#)
[Back](#)
[Close](#)
[Full Screen / Esc](#)
[Printer-friendly Version](#)
[Interactive Discussion](#)

## Saharan dust event impacts on cloud formation over Western Europe

M. Bangert et al.

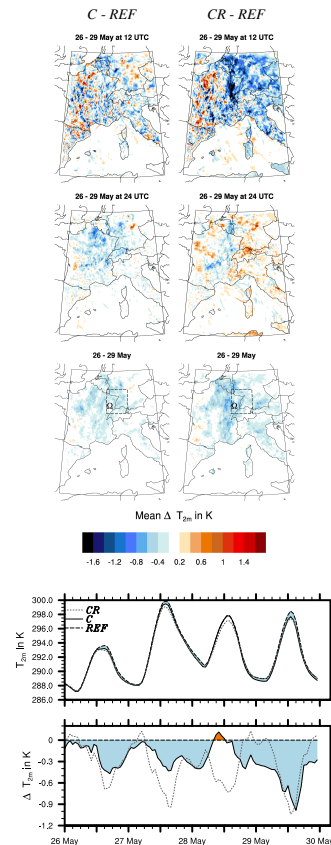


**Fig. 12.** Mean difference in  $T_{2m}$  at 12:00 UTC and 24:00 UTC from 26–29 May 2008 and total mean difference in  $T_{2m}$  from 26–29 May 2008 between simulation C and REF (top left column) and simulation CR and REF (top right column). Temporal evolution of  $T_{2m}$  and difference in  $T_{2m}$  with respect to case REF for area  $\Omega$  (bottom).